

Generating Semantic Adversarial Examples via Feature Manipulation

Shuo Wang, *Member, IEEE*, Tianle Chen, Shangyu Chen, Surya Nepal, *Member, IEEE*, Carsten Rudolph, *Member, IEEE* and Marthie Grobler, *Member, IEEE*,

Abstract—The vulnerability of deep neural networks to adversarial attacks has been widely demonstrated (e.g., adversarial example attacks). Traditional attacks perform unstructured pixel-wise perturbation to fool the classifier. An alternative approach is to have perturbations in the latent space. However, such perturbations are hard to control due to the lack of interpretability and disentanglement. In this paper, we propose a more practical adversarial attack by designing structured perturbation with semantic meanings. Our proposed technique manipulates the semantic attributes of images via the disentangled latent codes. The intuition behind our technique is that images in similar domains have some commonly shared but theme-independent semantic attributes, e.g. thickness of lines in handwritten digits, that can be bidirectionally mapped to disentangled latent codes. We generate adversarial perturbation by manipulating a single or a combination of these latent codes and propose two unsupervised semantic manipulation approaches: vector-based disentangled representation and feature map-based disentangled representation, in terms of the complexity of the latent codes and smoothness of the reconstructed images. We conduct extensive experimental evaluations on real-world image data to demonstrate the power of our attacks for black-box classifiers. We further demonstrate the existence of a universal, image-agnostic semantic adversarial example.

Index Terms—Adversarial examples, neural networks, feature manipulation, variational autoencoder, latent representation.



1 INTRODUCTION

The existence of adversarial examples causes serious security concerns about the reliability of deep neural networks (DNNs). In these adversarial examples, small perturbations that are hard for humans to recognize are intentionally added to the original inputs to cause a DNN to mislabel the perturbed inputs with high confidence [1], [2]. Most existing adversarial attacks are performed by adding unstructured perturbations only in the pixel-wise input space to fool the classifier. Such perturbations are often unnatural, not semantically meaningful and can easily be detected since they are distinctly identified in the latent space (far from the manifold of normal instances). Some recent works attempted to perturb the latent space, to obtain natural adversarial examples, e.g. [3]. However, due to lack of interpretability and disentanglement

Recent developments in variational autoencoder (VAE) [4]-based representation learning, e.g., β -VAE [5], FactorVAE [6], have resulted in significant advancements in the fields of disentanglement learning. These approaches provide an interpretable way to understand and control high dimensional data samples in terms of a low dimensional set of latent representations. Also known as disentanglement,

this is a representation where a change in one dimension corresponds to a change in one factor of variation while being relatively invariant to changes in other factors [7]. Consequently, it is feasible to conduct a new adversarial attack by manipulating disentangled latent representations (also called latent codes). Latent codes consist of a latent vector or a set of latent feature maps.

In this paper, we introduce a systematic framework to generate structured perturbation with semantic meanings to produce semantic adversarial examples with the smooth and natural visual transition while efficiently causing misclassification, by semantically connecting the disentangled latent space and the pixel input space. Demonstration is given in *Section 4.6 Attack Demonstration*. We assume that the images in similar domains have some commonly shared but theme-independent semantic attributes, e.g. thickness of lines in handwritten digits, that can be bidirectionally mapped to disentangled latent codes. We generate adversarial perturbation by manipulating a single or a combination of these latent codes, in an interpretable, smooth and stealthy manner. For example, we find a latent code that only controls the thickness of handwritten digits then we add perturbation to the corresponding factor encoded from a digit 7 to manipulate the thickness. This fools the classifier to misrecognize the perturbed digit as 1. Taking the face recognition as another example, the adversary can perform a semantic adversarial attack by identifying the disentangled latent code to reveal smiling facial expressions only. This could fool a face classifier to make the wrong prediction by conducting linear interpolation on the latent feature map to change a normal face with a smiling facial expression. The change of the adversarial example should be natural and smooth for humans.

- Shuo Wang is with the Faculty of Information Technology at Monash University and Data61 at CSIRO, Melbourne, Australia.
E-mail: shuo.wang@monash.edu
- Carsten Rudolph and Tianle Chen are with Faculty of Information Technology at Monash University, Melbourne, Australia.
E-mail: Carsten.Rudolph@monash.edu, tche119@student.monash.edu.
- Surya Nepal and Marthie Grobler are with Data61, CSIRO, Melbourne, Australia.
E-mail: Surya.Nepal@data61.csiro.au, Marthie.Grobler@data61.csiro.au.
- Shangyu Chen is with University of Melbourne, Melbourne, Australia.
E-mail: shangyuc@student.unimelb.edu.au.

In this work, we present generated adversaries to demonstrate the potential of the semantic adversarial attack for black-box classifiers, with the existence of an image-agnostic adversarial example. The main contributions of this work are summarized as follows:

(1) To obtain latent representation that can easily be manipulated in a human-cognition manner, we propose a common feature variational autoencoder (CF-VAE), with better disentanglement performance. CF-VAE is trained to obtain bidirectional mapping between the high-dimensional data samples x and the low-dimensional latent representation z (also called latent codes) that are disentangled and with semantic meaning. To achieve a better disentanglement, the CF-VAE divides the latent codes into theme-independent codes and theme-relevant codes. In addition, a Total Correlation term is used to improve independence in the distribution of latent code z to further improve disentanglement performance.

(2) To balance the trade-off and improve reconstruction quality, we propose a generative adversarial network-based booster (GAN-B) to learn a more accurate projection of mapping latent code to the pixel-wise domain. This is necessary since the utility of the reconstructed sample by the decoder is generally limited and blurry as a result of the trade-off between reconstruction and disentanglement. The feature-wise similarity is applied to transfer representation from pre-trained GAN (generative adversarial network) to the CF-VAE for reconstructing high-quality instances. Namely, the latent representation of a single layer l from the discriminator of GAN (trained on clean instances) is used as the reconstructed error evaluation for CF-VAE.

(3) We perturb the theme-independent codes to reconstruct an adversarial example that causes misclassification. It aims to find the optimal perturbation added to the specific factor of the latent code in a semantics-legible manner while ensuring the stealthiness of malicious perturbation in both a visual perspective and latent space so that it can defeat the latent detection-based defenses. The attack-effective value range for perturbation design that can effectively give rise to misclassification for a specific (or a combination) latent code is also recognized.

(4) We enhance the semantic adversarial attack against images with complex semantic attributes, e.g., face images, combining the CF-VAE with image-to-image translation. To obtain a better smoothness of perturbed images by reconstruction, we jointly train two CF-VAEs to obtain theme-independent latent codes, i.e. a set of feature maps, for semantic manipulation.

We conduct extensive experimental evaluations on the real-world image data to demonstrate the power of our attack for black-box classifiers and present a comprehensive empirical analysis of the possible factors that affect the attack. Our experiments reveal potential security breaches where adversaries can control the semantic features to break a classifier and demonstrate that semantic-based perturbation is more practical than pixel-wise manipulation. We also empirically investigate the universal semantic adversarial examples also exist.

The next section describes the preliminary concepts and the background on adversarial examples. Sections III and IV explain the system design and our approach. Section

V describes our experimental results. Section VI discusses related work, and Section VII concludes the work as a whole.

2 BACKGROUND

2.1 Adversarial Examples

For a given input sample x , the adversarial example [8] is a sample x' that is similar to x (according to particular measure metrics) but so that the decision of the classifier \mathcal{F} $\mathcal{F}(x) \neq \mathcal{F}(x')$ [9]. A classifier can misclassify an adversarial example for two reasons. (1) The adversarial example is far from the boundary of the manifold of the task. For example, the task is a handwritten digit classification, and the adversarial example is an image containing no digit, but the classifier has no option to reject this example and is forced to output a class label. (2) The adversarial example is close to the boundary of the manifold. If the classifier poorly generalizes the manifold in the vicinity of the adversarial example, then misclassification occurs.

2.2 Generative Adversarial Networks

The typical GAN architecture contains two neural networks: one generator neural network G , trained to generate a sample from a set of random numbers, and one discriminator D , trained to categorize data as real or fake. As the GAN networks are trained, G learns to generate samples that can fool D . Let $p_z(z)$ be the input noise distribution of G and $p_{data}(x)$ be the real data distribution, the purpose of GANs is to train G and D to play the following two-player minimax game with value function $V(G, D)$:

$$\min_G \max_D V(G, D) = E_x \sim p_{data}(x) [\log D(x)] + E_z \sim p_z(z) [\log(1 - D(G(z)))] \quad (1)$$

GAN can be applied in varied unsupervised and semi-supervised learning tasks [10], [11], [12], [13], [14].

2.3 Autoencoders and β -VAE

Autoencoders (AEs) are common deep models in unsupervised learning [7]. They aim to represent high-dimensional data through the low-dimensional latent layer, a.k.a. bottleneck vector or code. Architecturally, Basically, an encoder E , parameterized by $q_\phi(z|x)$, is trained to convert high-dimensional data x into the latent representation bottleneck vector z in latent space that follows a specific Gaussian distribution $p(z) \sim N(0, 1)$. The decoder $p_\theta(x|z)$ is trained to reconstruct the latent vector z to x . The training process of the autoencoders is to minimize the reconstruction error. Formally, we can define the encoder and the decoder as transitions τ_1 and τ_2 :

$$\tau_1(X) \rightarrow Z, \tau_2(Z) \rightarrow \hat{X}, \tau_1, \tau_2 = \underset{\tau_1, \tau_2}{\operatorname{argmin}} \left\| X - \hat{X} \right\|^2 \quad (2)$$

The VAEs model [4] shares the same structure with the autoencoders but is based on an assumption that the latent variables follow some kind of distribution, such as Gaussian or uniform distribution. It uses variational inference for the learning of the latent variables. In VAEs the hypothesis is that the data is generated by a directed graphical

model $p(x|z)$ and the encoder is to learn an approximation $q_\phi(z|x)$ to the posterior distribution $p_\theta(z|x)$ estimated by the decoder. The encoder and decoder are trained simultaneously based on the negative reconstruction error and the regularization term, i.e., Kullback-Leibler (KL) divergence between $q_\phi(z|x)$ and $p(z)$, by optimizing the variational lower bound:

$$L(\theta, \phi; x) = KL(q_\phi(z|x)||p(z)) - \mathbf{E}_{q_\phi(z|x)}[\log p_\theta(x|z)] \quad (3)$$

The left part is the KL divergence regularization term to match the posterior of z conditional on x , i.e., $q_\phi(z|x)$, to a target distribution $p(z)$, e.g., Gaussian distribution whose mean μ and diagonal covariance Σ are the encoder output.

The right part denotes the reconstruction loss for a specific sample x . In a training batch, the loss can be averaged as:

$$\begin{aligned} L_{VAE} &= \mathbf{E}_{p_{data}(x)}[L(\theta, \phi; x)] \\ &= \mathbf{E}_{p_{data}(x)}[KL(q_\phi(z|x)||p_\theta(z))] - \mathbf{E}_{p_{data}(x)}[\mathbf{E}_{q_\phi(z|x)}[\log p_\theta(x|z)]] \end{aligned} \quad (4)$$

β -VAE [5] is a modification of the VAE framework that introduces an adjustable hyperparameter β to the original VAE objective:

$$\mathcal{L} = \mathbf{E}_{q_\phi}(\log p_\theta(x|z)) - \beta D_{KL}(q_\phi(z|x)||p_\theta(z)) \quad (5)$$

Well chosen values of β (usually $\beta > 1$) result in more disentangled latent representations z . Therefore, there exists a value of $\beta > 1$ that gives the highest disentanglement but results in a higher reconstruction error than a VAE.

3 PROBLEM DEFINITION

3.1 Semantic Adversarial Example

Unlike the notion of the adversarial example introduced in Section 2, the semantic adversarial example can be defined and formalized as follows.

Let D denote the set of examples in the sample space. Let $\mathcal{F}(x)$ denote a pre-trained classifier, which outputs the final prediction label $y = \mathcal{F}(x)$. Let S denote the set of underlying semantic features, interpreted as the representation of the data by human cognition. For example, $s_1 \in S$ is the color of skin and $s_2 \in S$ is the length of hair for a given human face image. We assume that observations $x \in D$ can be generated by combining M primary disentangled latent factors $S_o = (s_1, \dots, s_M)$, $s_i \in S$, and $S_c = (s_1, \dots, s_K)$, $s_i \in S_o$ is the set of K commonly shared or theme-independent features across classes, e.g. the thickness of handwritten digits or facial express of face images. Unlike most existing adversarial examples that directly add unstructured pixel-wise perturbation in the input space or random latent representation of z space, our adversary A aims at perturbing a fraction of disentangled latent representations derived from a sample x to generate structured perturbations with semantic meaning, e.g. changing the thickness of digits or the facial expression of face images. Such semantic perturbation is named semantic feature manipulation, which is achieved by (1) learning a latent code that can reveal the commonly shared or theme-independent features across classes, e.g., via VAE-based disentangled learning; (2) perturbing latent codes to reconstruct an adversarial example that can fool a targeted classifier in an interpretable, natural and smooth manner.

Formally, let $E(x)$ be an encoder that can map x to latent codes \vec{z} , namely $E(x) \rightarrow \vec{z} = \{z_1, \dots, z_M\}$, in which z_i reveals a specific semantic feature s_i and z_i follow the distribution P_z . \vec{z} can be inverted back to x^* with the help of a decoder $D(\vec{z}) \rightarrow x^*$. The perturbation of latent codes is to add random noise Δz to the values of the latent codes, assuming z_i for simplicity. Δz is from the same distribution P_z as z . The goal of A is to design perturbation Δz for z_i to fool the pre-trained classifier f such that $\mathcal{F}(x^*) \neq y$, $D(E(x) = \{z_1, \dots, z_i + \Delta z, \dots\}) \rightarrow x^*$ while Δz to be imperceptible and x^* to be as similar as x (according to particular smoothness metrics).

The adversarial image x^* for x can be designed by satisfying the three objectives given as follows, with respect to the reconstructed image based on the perturbed latent codes.

$$\begin{aligned} x^* &= D(E(x) = \{z_1, \dots, z_i + \Delta z^*, \dots\}), \\ &\text{s.t. } \mathcal{F}(x^*) \neq y \text{ and } \|\Delta z^*\| \leq \epsilon, \\ &\Delta z^* = \operatorname{argmin} \|\Delta z\|, \end{aligned} \quad (6)$$

and $\text{similarity}(x^*, x) \geq \theta_{SIM}$

The universal definition of the semantic adversarial example is defined as follows: Let D^y denote the set of examples with the same label y , the perturbation Δz , added in a specific latent factor z_i on a $x \in D^y$ to make misclassification, can also cause misclassification on a number of other $x' \in D^y$. The fraction of the affected instance is referred to as the fooling rate (FR). Namely, for the universal adversarial semantic adversarial example, not only the above equation should be satisfied but the fooling rate should also be more than a threshold $FR_{\Delta z^*}^{D^y} \geq \theta_{FR}$.

3.2 Adversary Model

We characterize an adversary according to its goals and knowledge regarding the learning model and training data.

3.2.1 Goals

To launch an effective and successful semantic adversarial attack, the following goals of the adversary should be satisfied.

(G1) Efficient perturbation to fool target classifier (term 1 in Eq. 6). A successful attack must have a high and consistent success rate (SR). The adversarial perturbation should be sufficiently reliable that a given perturbed instance is classified with high accuracy to the wrong label. A non-targeted misclassification attack is explored in this work. To ensure the consistent nature of the SR, the proportion of satisfactory perturbations that give rise to misclassification in high probability, within an interpolation value range $[low, high]$, a.k.a efficient ratio ER , should be more than a threshold θ_{ER} ;

(G2) Stealthy perturbation. It is desirable that the adversarial perturbation is stealthy so that it is hard to detect and should be visually imperceptible both in input space and latent space, even under the examination of a machine detector. Invisible perturbation should be added in the latent code so that the perturbed instance is close to the manifold of normal data in latent space (invisible/imperceptible, term 2 in Eq. 6), namely $|\Delta z_i^*|_p \leq \epsilon$.

(G3) The perturbed instance has a high level of semantic similarity with the original instance, i.e., the change of the instance in the input space is considered as natural and smooth to the human eye (stealthiness, term 3 in Eq. 6), namely $Similarity(x^*, x) \geq \theta_{SIM}$;

(G4) Perturbation should be as universal as possible, i.e., a single perturbation Δz^* can affect multiple instances, namely, the fooling rate should be more than θ_{FR} . It is desirable that the adversarial perturbation is universal so that it is easy to design an effective perturbation for a large database without time and resource overheads.

3.2.2 Knowledge

In contrast to the minimal knowledge assumption that the adversary has known neither the training data nor the specifics of the learning model, we relax some of the assumptions related to the attacker’s knowledge. Here, we assume that the adversary has no knowledge of the model architecture, i.e., black-box classifier, but has access to the training data, or either can know the type of training data the targeted classifier used, e.g., human face data or can obtain some very relevant data.

4 FRAMEWORK FOR GENERATING SEMANTIC ADVERSARIAL EXAMPLE

In this paper, we propose a semantic adversarial attack scheme that is interpretable, smooth and universal. In this section, we describe the two approaches of our attack scheme: *Vector-based Semantic Manipulation* and *Feature Map-based Semantic Manipulation*, and its three main components, *Learning Disentangled Representations*, *GAN-Based Booster* and *Invisible Latent Perturbation*.

4.1 Attack Overview

Our attack scheme aims to generate interpretable and universal semantic adversarial examples with invisible perturbation by manipulating some commonly shared or theme-independent features. Ideally, we can learn a disentangled latent code vector that can be used to reconstruct images and one factor of the vector affects one semantic feature only, via solely conducting naive common feature variational autoencoder(CF-VAE).This may work well for simple images (e.g. handwriting digits), as the diversity and dimension of the feature are simple and most of the essential features can be captured via a 20-dimensional vector. However, the quality of the reconstructed image is significantly affected by the diversity and dimension of the feature retained by the latent codes, as well as the trade-offs between the disentanglement performance and the reconstruction quality. The performance on the complex images (e.g. face) is not as good as the simple images (e.g. handwriting digits) when only conducting onefold CF-VAE, since the feature dimension of the face is very large, and it is hard to leverage a low-dimensional latent code vector to generate a natural and smooth perturbed image.

Therefore, we apply two semantic manipulation approaches to generate adversarial instances in terms of the feasibility of semantic manipulation: *Vector-based Semantic Manipulation via Onefold CF-VAE* and *Feature Map-based Semantic Manipulation via Multiple CF-VAE*. The advantage of

the onefold approach is the unsupervised manner and that no corresponding image pairs are required. The advantage of the multiple approaches is the precise constraint on reconstituted images to achieve better quality.

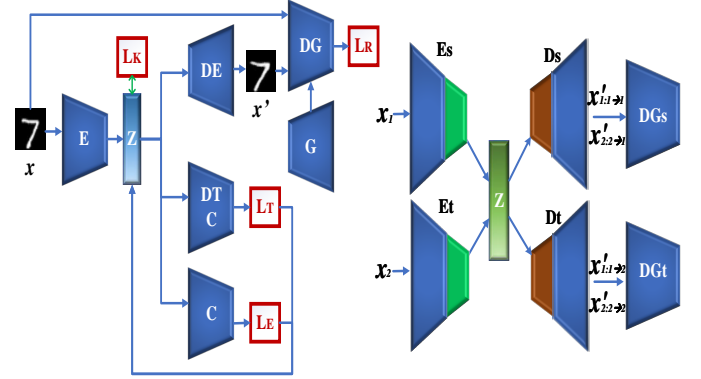


Fig. 1. The vector-based semantic manipulation scheme via onefold CF-VAE (left) and feature map-based semantic manipulation scheme via multiple CF-VAEs (right). The loss function of the CF-VAE combines L_K , L_R , L_T and L_E . DTC (Discriminator for TC estimation) is trained to estimate the TC value, C is trained to strip class-unique features and DG (Discriminator of GAN) improves the reconstruction error evaluation.

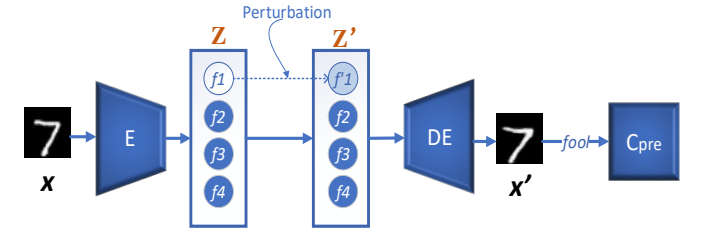


Fig. 2. The semantic adversarial example perturbation scheme. Given an instance x , semantic adversarial attack generates adversarials by perturbing disentangled latent factor(s) and decoding the perturbation’s latent bottleneck vector to fool the pre-trained classifier C_{pre} .

Vector-based Semantic Manipulation via Onefold CF-VAE. This can be implemented by a sole CF-VAE based representation learning, as shown in Fig.1 left, trained on clean training samples to obtain disentangled and independent latent representations that are easy to control and understand by humans. To improve the disentanglement performance, a discriminator is trained for Total Correlation (TC) [15] estimation (DTC) to improve the independence of latent representations for CF-VAE. In addition, a classifier C is trained to filter class-unique information and only retain the common features to further improve the disentanglement performance. To improve the reconstruction quality, a generative adversarial network-based booster (GAN-B) is trained on clean training instances, which provides a discriminator DG to improve the reconstruction error evaluation so that it enhances the quality of reconstructed instances. Finally, an invisible latent perturbation by stochastic searching is used to seek perturbation $z'_i = z_i + \Delta z$ for a specific disentangled latent factor z_i (or a group), to achieve the adversarial goals, as shown in Fig. 2. Details of each component will be introduced in the following sections.

Feature Map-based Semantic Manipulation via multiple CF-VAE. For the complex images, we apply an unsupervised image-to-image translation, e.g. UNIT or MUNIT [16], [17],

to learn the theme-independent latent codes for semantic manipulation. We learn the desired semantic attribute-conditional transition from well-labeled natural images, e.g. CelebA [18] or RaFD dataset, for semantic manipulation. For instance, a set of smiley face images can be considered as a smile domain, the semantic transition from a natural face to smile can be conducted by learning a joint distribution of images in source and targeted (smile) domains. In this scenario, we assume that for any given pair of corresponding images (x_s, x_t) in source and targeted domains, X_s and X_t , can be mapped to the same latent representation in commonly shared latent codes z [16]. Here, the code is a set of feature maps, i.e. blocks of a feature matrix. Namely, both images can be recovered from this code, and we can compute this code from each of the two images. To achieve this goal, we jointly train two CF-VAEs on the source images X_s (to attack) and target image X_t (to change for, e.g., smile face images), as two domains, as shown in Fig. 1 right. Consequently, we can use $D_t(z_s \sim q_s(z_s|x_s))$ to translate images from X_s to X_t by assembling a subset of the subnetworks. GAN-B can be also incorporated into the image-to-image transition to improve the quality of the reconstructed images. The latent code’s iteratively stochastic searching is applied to generate adversarial examples by perturbing the shared latent codes (a set of the matrix) that control the desired semantic attributes.

4.2 Vector-based Semantic Manipulation via onefold CF-VAE

For images with a small number of semantic attributes, a low-dimensional latent code vector, learned by a onefold VAE-based disentanglement learning, can maintain most of the significant features of images. Then, it is desired to obtain better disentangled and theme-independent latent codes, which will be used to design smooth and natural adversarial examples via semantic manipulation-based perturbation. Consequently, we propose CF-VAE, derived from VAE. It is incorporated with a classifier on top of the latent code to achieve disentanglement in the latent codes z that follow a fixed prior distribution while being unrelated to the label, i.e. to extract class irrelevant z . Furthermore, Total Correlation (TC) [15] is applied to promote the latent factors to be more independent, to improve the disentanglement performance.

4.2.1 Disentangled theme-independent code learning

To obtain theme-irrelevance for good disentanglement in z , we apply the irrelevance term L_E , estimated by a classifier parameterized by ς on the latent codes z , derived from the encoder $q_\phi(z|x)$, to classify the label of z . The adversarial learning approach, similar to [19], is used to train the classifier. The adversarial classifier is added after z to distinguish its label, while the encoder tries to fool it, as demonstrated in Fig. 1 left. The objective of the classifier can be defined as cross-entropy loss:

$$L_C = -E_{q_\phi(z|x)} \sum_c I(c=y) \log q_\varsigma(c|z) \quad (7)$$

Here $I(c=y)$ is the indicator function, and $q_\varsigma(c|z)$ is softmax probability output of the classifier. Simply, we

assume the labels are distributed uniformly across all inputs, i.e. class probabilities $\pi = 1/C$. To peel the effect of labels and to extract class irrelevant z , the encoder $q_\phi(z|x)$ is simultaneously trained to fool the classifier with loss added by a cross entropy loss defined as follows:

$$L_E = E_{q_\phi(z|x)} \sum_c \frac{1}{C} \log q_\varsigma(c|z) \quad (8)$$

4.2.2 Disentanglement improvement by inner-independence

To obtain inner independence for good disentanglement in z , Total Correlation (TC) [15] is used to encourage independence in the latent vector z , formally

$$TC(z) = KL(q(z)||\bar{q}(z)) = Eq(z)[\log \frac{q(z)}{\bar{q}(z)}] \quad (9)$$

As TC is hard to obtain, the approximate tricks used in [6] is applied to estimate TC. Specifically, a discriminator DTC is applied to output an estimate of the probability $D(z)$ whose input is a sample from $q(z)$ rather than from $\bar{q}(z)$ to classify between samples from $q(z)$ and $\bar{q}(z)$, thus learning to approximate the density ratio needed for estimating TC [6]. DTC , parameterized by v , is trained with the other CF-VAE components jointly. Thus, the TC term is replaced by the discriminator-based approximation as follows:

$$L_T = TC(z) \approx E_{q(z)} [\log \frac{D(z)}{1-D(z)}] \quad (10)$$

4.2.3 Onefold CF-VAE Training

The objective of CF-VAE is augmented with a TC [15] term and L_E to encourage independence in the latent factor distribution, given as follows:

$$\frac{1}{N} \sum_N^{i=1} [E_{q_\phi(z|x^{(i)})} [\log p_\theta(x^{(i)}|z)] - D_{KL}(q_\phi(z|x^{(i)})||p(z))] \quad (11)$$

$$-\gamma L_T - L_E$$

This is also a lower bound on the marginal log likelihood $E_{p(x)}[\log p(x)]$. The first part reveals the reconstruction error, denoted by L_R , evaluating whether the latent codes z is informative enough to recover the original instance, e.g., l_2 loss between the original instance and the reconstructed instance. The second part is a regularization term, denoted by L_K , to push $q_\phi(z|x)$ to match the prior distribution $p(z)$. The third part is the TC term, denoted by L_T (Equation 10), to measure the dependence for multiple random variables. The last part is the irrelevance term L_E (Equation 8).

The parameter ϕ of encoder $q_\phi(z|x)$ is then trained by L_K, L_E, L_R and L_T in terms of $-\nabla_\phi(-L_R + L_K + \gamma L_T + L_E)$, to let z be unrelated to the label, independent of each other and close to $N(0, I)$. The parameter ς of the adversarial classifier is updated in terms of $-\nabla_\varsigma(L_C)$. The parameter θ of decoder is updated in terms of $-\nabla_\theta(L_R)$. The parameter v of adversarial classifier is updated in terms of $-\nabla_v(L_T)$, i.e. $-\nabla_v \frac{1}{2|B|} [\sum_{i \in B} \log(D_v(z^{(i)})) + \sum_{i \in B'} \log(1 - D_v(\text{permutedim}(z'^{(i)})))]$ [6]. Here, the permutedim function is to random permute on a sample in the batch for each dimension of its z .

4.3 GAN-Based Booster

To address the trade-off between the reconstruction and disentanglement, we apply a GAN-based booster. Specifically, the GAN discriminator is used to learn a comprehensive similarity metric to discriminate real images from fake images. Inspired by [4], [20], the feature-wise metric expressed in the GAN discriminator, a.k.a. style error or content error is used as a more abstract reconstruction error L_R for VAE to better measure the similarity between the original instance and the reconstructed image, aiming to improve the utility of the reconstructed instance. That is, we can use learned feature representations in the discriminator of a pre-trained GAN as the basis for the VAE reconstruction objective.

Specifically, let x and \hat{x} be the original image and the reconstructed image and $F^l(x)$ and $F^l(\hat{x})$ be their respective hidden feature representation of the l^{th} layer of the discriminator, the representation loss to reveal reconstruction error is defined in Eq. 12 and 13. A Gaussian observation model is applied for $F^l(x)$ with mean $F^l(\hat{x})$ and identity covariance $p(F^l(x)|z) = N(F^l(x)|F^l(\hat{x}), I)$.

$$L_{rec}^{F^l} = -E_{q(z|x)}[\log p(F^l(x)|z)] \quad (12)$$

$$L_{rec}^{content}(x, \hat{x}, l) = \frac{1}{2} \sum_{i,j} (F_{i,j}^l - \hat{F}_{i,j}^l)^2 \quad (13)$$

Simply, a GAN is trained in original clean instances. A single layer l is then chosen from the discriminator network and used to obtain representation similarity according to $F^l(x)$. The CF-VAE is then trained based on the representation error, leveraging the learned feature representations in the discriminator as the basis for the VAE reconstruction objective. Note that another variant of GAN, such as info-GAN [10], can be directly incorporated into our framework.

4.4 Invisible Latent Perturbation by Stochastic Searching

In this section, we introduce an invisible perturbation approach to manipulate the latent codes $z_i \in z$ of an instance x , where $E(x) \rightarrow z$. We construct minimum perturbations $z_i^* = z_i + \Delta z^*$ to reconstruct adversarial samples $x^* = D(\hat{z} = \{\dots, z_i^*, \dots\})$ that can fool a classifier into making wrong predictions over a number of instances with the common feature controlled by z_i .

For simplicity, only one latent code factor is considered to be perturbed at one time. Let \mathcal{F} be a neural network classifier to be attacked and D be a set of training data samples for \mathcal{F} or similar detests. The perturbation mechanism iterative goes through each sample $x \in D$, and searches for the optimal perturbation in the neighborhood of $z_i \in E(x) = z$, within a searching range $[r, r + \Delta r]$ for z_i , to achieve misclassification and satisfy goals G1-4 in Section III-B.

At each searching iteration, N perturbations Δz_i are randomly sampled within the current search range for evaluation. Effective Ratio (ER) is used as the indicator to evaluate the effectiveness of perturbation, defined as follows:

$$ER = \frac{1}{N} \sum_{i=1}^N 1_{\mathcal{F}(D(E(x)z_i)) \neq \mathcal{F}(x)} \quad (14)$$

To satisfy G1, misclassifications should be commonly achieved, i.e. ER exceeds a threshold θ_{ER} . G2 is satisfied by the constraint of the searching range $\|r + \Delta r\| \leq \epsilon$, where the updated perturbation is searched within the L_p ball of radius r , $\Delta z_i \sim (r, r + \Delta r)$. To satisfy G3, the structural similarity (SSIM) [21] between the original input and the reconstructed instance should exceed a threshold of θ_{SSIM} . The search range of perturbation $(r, r + \Delta r)$ that is incrementally raised by Δr , until G1 to G3 are satisfied simultaneously. Among Δz_i^* , the one that has the closest distance to the original z_i , is selected to reconstruct x^* for x_i as the adversarial example.

For the universal perturbation, the iterative searching is further evaluated in terms of universality on a set of data samples in the given class y , D^y , namely to evaluate whether a Δz_i^* from the previous steps satisfies the G4. Specifically, for each Δz_i^* that satisfies G1-G3 simultaneously, its universality will be further evaluated using the universal indicator, fooling rate (FR), defined as follows:

$$FR = \frac{1}{m} \sum_{i=1}^m 1_{\mathcal{F}(D(E(x_m)z_i)) \neq \mathcal{F}(x_m)} \quad (15)$$

Here, the validation dataset is $X_{\Delta z^*, z_i} = \{D(E(x_1)z_i + \Delta z^*), \dots, D(E(x_m)z_i + \Delta z^*)\}$ modified from a batch of m samples of D^y . The searching is terminated when the empirical FR on the $X_{\Delta z^*, z_i}$ exceeds the target threshold θ_{FR} . The detailed algorithm is given in Algorithm 1.

Algorithm 1: Invisible Latent Perturbation Algorithm

Input: an instance x , search start value r and upper bound r_{max} , ϵ , target black-box classifier f , specific latent factor z_i , pre-trained encoder E and decoder DE from CF-VAE+GAN-B, threshold $\theta_{ER}, \theta_{FR}, \theta_{SSIM}$.

Output: Universal perturbation Δz^*

```

1 S= $\emptyset$ 
2  $y = f(x), z = E(x), r=0$ 
3 while  $FR < \theta_{FR}$  or  $r + \epsilon < r_{max}$  do
4    $\{\Delta z\} \leftarrow$  sample N random noise within  $[r, r + \epsilon]$ 
5   count = 0
6   for  $\Delta z$  in  $\{\Delta z\}$  do
7      $z'_i = z_i + \Delta z, \hat{x} = DE(\hat{z}), \hat{y} = f(\hat{x})$ 
8     if  $\hat{y} \neq y$  then
9       count ++, S.add( $\Delta z$ ), SIM= $similarity(\hat{x}, x)$ 
10     $X_{new} \leftarrow$  sample M instances from X
11     $FR = \frac{1}{M} \sum_{i=1}^M 1_{\hat{x} \neq y, x_i \in X_{new}}$ 
12  ER=count/N
13  if  $SIM < \theta_{SSIM}$  or  $ER < \theta_{ER}$  then
14     $r = r + \epsilon$ 
15  else
16     $\Delta z^* = argmin_{\Delta z \in S}$ 

```

4.5 Feature Map-based Semantic Manipulation via multiple CF-VAE

To achieve semantic manipulation via image-to-image transition for the manipulation of complex images, two encoders E_s and E_t of CF-VAE are applied for mapping images to the same latent codes, while two decoders D_s and D_t are used to map latent codes to images in two domains, respectively.

Given corresponding images pair (x_s, x_t) from the joint distribution, then $z = E_s(x_s) = E_t(x_t)$ and conversely $x_s = D_s(z)$ and $x_t = D_t(z)$. The attribute-conditional semantic manipulation can be achieved via learning the function $x_t = F_{s \rightarrow t}(x_s) = D_t(E_s(x_s))$ to map from X_s to X_t . Such shared codes assumption implies the cycle-consistency assumption [22], i.e. $x_s = F_{t \rightarrow s}(F_{s \rightarrow t}(x_s))$. These two CF-VAE are implemented based on the shared-latent space assumption using a weight sharing constraint [16] and cycle-consistency (CC) [22]. The weight-sharing constraint is used to relate the two CF-VAEs.

Specifically, the connection weights of the last few layers in E_s and E_t are shared to extract high-level representations of the input images in the two domains. Likewise, the connection weights of the first few layers in D_s and D_t are shared to decode high-level representations for reconstructing the input images. When a pair of corresponding images can be well mapped to the same latent code and this same latent code is decoded to a pair of corresponding images, image-to-image translation occurs, i.e. an image x_s in X_s is translated to an image in X_t . This can be conducted through applying $D_t(z_s \sim q_s(z_s|x_s))$. The $X_s \rightarrow X_t$ and $X_t \rightarrow X_s$ can be trained jointly. In addition, we enforce the CC constraint in this joint training to further regularize the ill-posed unsupervised image-to-image translation problem.

The learning object is given as follows:

$$\begin{aligned} \min_{E_s, D_s, E_t, D_t} & L_{VAE_s}(E_s, D_s) + L_{CC_s}(E_s, D_s) + L_{GAN_s}(E_t, D_s, DG_s) \\ & + L_{VAE_t}(E_t, D_t) + L_{CC_t}(E_t, D_t) + L_{GAN_t}(E_s, D_t, DiSt_t) \end{aligned} \quad (16)$$

The VAE objects are the same with Equation 11. The GAN objective functions are given by conditional GAN objective functions:

$$\begin{aligned} L_{GAN_s}(E_t, D_s, DiS_s) &= \lambda_g E_{x_s \sim P_{X_s}}[\log DiS_s(x_s)] \\ &+ \lambda_g E_{z_t \sim q_t}(z_t|x_t)[\log(1 - DiS_s(D_s(z_t)))] \\ L_{GAN_t}(E_s, D_t, DiSt_t) &= \lambda_g E_{x_t \sim P_{X_t}}[\log DiSt_t(x_t)] \\ &+ \lambda_g E_{z_s \sim q_s}(z_s|x_s)[\log(1 - DiSt_t(D_t(z_s)))] \end{aligned} \quad (17)$$

GAN objective functions are applied to ensure that the translated images resemble images in the target domains, respectively, using λ_g to control the impact of the GAN objective functions. The CC constraint is modeled via a VAE-like objective function, similar to [16]. If we jointly train the GAN with the VAE, this can be conducted by solving a mini-max problem, as in [4]. Consequently, we can use $D_t(z_s \sim q_s(z_s|x_s))$ to translate images from X_s to X_t by assembling a subset of the subnetworks.

A latent code iterative stochastic searching is then applied to generate adversarial examples, similar to Algorithm 2. Note that, as the dimension of the latent codes can be very large in this scenario, they are stored as a set of feature map (matrix), e.g., a set of 256 feature matrix with $64 * 64$ elements. We treat each matrix as a latent factor, then Δz can be selected as the same value for each element of the matrix and the searching range is a L_{64*64} ball of radius r .

4.6 Attack Demonstration

In this section, two types of semantic adversarial examples are demonstrated, using the vector and feature map based semantic manipulation, respectively. A synthetic semantic

adversarial example on the handwritten digits of MNIST [23] is shown in Fig. 3, which is used to demonstrate that an adversarial digit image can be designed by modifying only one latent code so that the change looks like something a person would write in order to fool both a classifier and human.

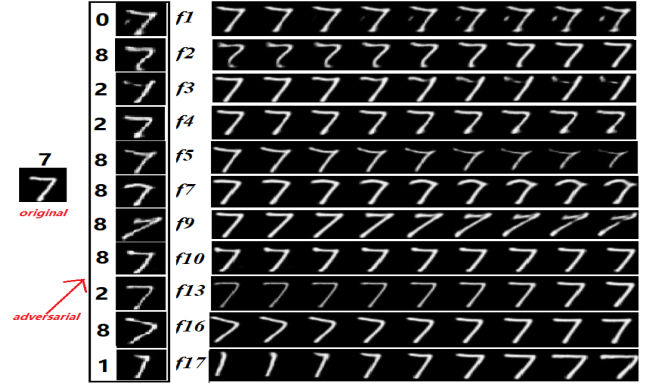


Fig. 3. Semantic adversarial examples of MNIST. The figure to the left is the original digit "7" instance. Figures in the second part are perturbed instances that make misclassification (labels in front) by changing only one specific latent variable (f_n). Figures in the third part are the reconstructed instances, created by changing one latent variable on the original instance.

Specifically, an adversary trains a CF-VAE on a publicly-available handwritten digits dataset and applies the encoder of the CF-VAE to effectively map instance x to its corresponding latent bottleneck vector z composed of 20 disentangled latent codes. Then the adversary will choose some specific latent factor(s) from the latent code vector z to conduct perturbation, which has been given semantic meanings. The perturbed latent vector can be reconstructed to x' with the help of the decoder. There are 11 disentangled latent factors selected in Fig. 3 in terms of semantic meaning, e.g. f_7 , f_9 , f_{13} , f_{16} , f_{17} respectively represent the degree of horizontal stroke crook, turning angle, thickness, rotation, and horizontal scale. Due to the disentanglement representation, each latent factor is exclusively responsible for the variation of a unique feature in the observed data. The perturbation on the factor will not significantly change the perceived quality of the original instance (e.g., it would look like a natural person's handwriting) and the reconstructed x' should be similar to the original instance yet mislead classifiers' decision behavior on the input.

It is easy to perturb each (or a group) latent variable to conduct the misclassification for the adversary in a human-cognition way. Taking the digit "7" in Fig. 3 as an example, changing the value of latent variable f_7 (degree of horizontal stroke crook) could fool LeNet [24] (test accuracy 99.1%) to change the label 7 to others. The latent codes that enable misclassification and retain the perceived quality of the reconstructed instance will be selected to conduct an attack in a more practical way, i.e., f_4 , f_7 , f_{10} , f_{13} . Furthermore, the adversary can add the same perturbation to the same latent factor for other "7" digits to evaluate the fooling ability and find a universal perturbation that causes misclassification generally for all "7" digits.

We also provide a synthetic semantic adversarial example demonstrated on the CelebA [25] database using the feature map based semantic manipulation, as shown in Fig.



Fig. 4. Semantic adversarial examples of CelebA. The figure on the left is the original face instance. Figures in the middle are the instances reconstructed by conducting linear interpolation with the same perturbation on each latent matrix of the original instance. The figures in the part on the right are perturbed instances that lead to misclassification by changing only one specific latent matrix that reveals a specific semantic features only.

4. The adversary jointly trains two CF-VAEs on the clean training samples or relevant source dataset (e.g., CelebA) and target dataset (e.g., only smile face in RaFD or CelebA), treated as the image-to-image transition. Then the input face image can be mapped into $256 \times 64 \times 64$ -dimensions latent codes, i.e. feature map, using the encoders of these two CF-VAEs. We find that some 64×64 -dimensions matrices can reveal some disentangled semantic features. For example, we choose four matrices that respectively represent the degree of face light, smiling expression, beard and age, in Fig. 4. The adversary can choose a latent matrix that only impacts one specific semantic meaning, to conduct the semantic manipulation-based perturbation. Then the adversary will find an invisible and efficient perturbation for each selected latent factor, to cause the targeted classifier to misclassify the reconstructed instance. For example, the adversary can add perturbation to the second latent matrix to only change the smiling degree until the reconstructed face is misclassified. Furthermore, the adversary can add the same perturbation to the same latent matrix for other face images of this person to evaluate the fooling ability and find a universal perturbation that causes misclassification in general for this person.

5 EXPERIMENTS

5.1 Datasets

In this section, we present the results from the empirical evaluations of the proposed approach over two types of benchmark datasets. (1) MNIST [23] consists of 28×28 grayscale handwritten digit images from 10 classes, i.e., digit 0-9 and has a training set of 55000 instances and a test set of 10000 instances. (2) CelebA (cropped version) [25] consists of 202,599 RGB $64 \times 64 \times 3$ images of various celebrities, including 10,177 unique identities and 40 binary attribute annotations per image.

5.2 Metrics

In this section, we evaluate the effectiveness of our proposed adversarial attack with experimental results on images. We rely on the following measures.

5.2.1 Success Rate (SR)

SR aims to measure the fraction of perturbed samples drawn from the test set being classified as the target class in the case of a targeted attack, changing to other arbitrary target class in the case of non-targeted attacks. A high SR shows an effective ability of the adversarial example to fool the classifier. SR is used to evaluate the vulnerability of trained classifiers to our semantic adversarial attack.

5.2.2 Perturbation Stealthiness

The stealthiness of perturbation represents the quality of the perturbation to generate an adversarial example. Although the perturbed samples with perturbation are likely visually imperceptible, it is preferable for the perturbation to be also imperceptible in latent space and evade input-preprocessing defenses. Therefore, three quantitative measurements are implemented to evaluate the stealthiness of semantic adversarial example via perturbation. (1) Perceptual Hashing (pHash) Similarity: pHash [26] is used to present the fingerprint of an image based on its features. The pHash can measure the overall feature representation, instead of measuring the abrupt pixel change of an image. Images with similar features have similar pHash value. We can use the following equation to determine the similarity between the original image and the perturbed image and estimate how much the original image has been changed.

$$S_{image} = \left(1 - \frac{HD(pHash_{ori}, pHash_{poi})}{64}\right) \times 100\% \quad (18)$$

where HD is the Hamming Distance, and 64 represent the binary length of the pHash score.

(2) Structural Dissimilarity (SSIM). This is used to measure the internal feature similarity as a distance matrix evaluating the structural similarity of images [21]. It is closer to the human sensitivities compared to L_p distance. Therefore, using SSIM to evaluate the difference between two images satisfies human criterion more about negligible perturbation. It evaluates the difference between two input images similar to human’s criterion which is suit for the two image recognition applications in our experiments.

(3) Distance in the latent space (DLS). The difference in the input x representation between the instance and its corresponding adversarial example, e.g., RMSE of the pixels, is not enough to quantify the semantic distance underlying them. Therefore, we use the distance in the latent space between them, i.e., $\Delta z = \|z^* - z'\|$, to evaluate how much each instance is changed to achieve misclassification.

(4) The mean-squared error (MSE) between two images is used as the pixel-wise similarity measure.

5.3 Setup

We evaluated our attack when two strong defenses are present. One feasible defense against our attack is to train the same autoencoder using relevant data and then find the normal value range for each disentangled feature factor. The adversary and protector are considered two parties of a game. The common parameter for defending and attacking in this game is the threshold to decide the normal value. The varying threshold of distance in the latent space (DLS) is used to reveal different levels of distinguishability of

defenses. Another defense is the input-based de-noising by a threshold of the pixel-wise reconstruction error. Therefore, we use the mean-squared error (MSE) between original and reconstructed instance to reveal the robustness of our attack against such defenses; the varying threshold of MSE represents different levels of distinguishability of defenses. This can be considered as a general input-based defense, e.g., Magnet.

An existing similar adversarial attack on latent space is [3], in which the latent vector is not perturbed in an interpretable manner and without controllable mapping from latent space to pixel space. We simplify this type of attack as a general latent perturbation in our experiments, in which the latent vector is perturbed randomly. We compare our semantic attack with this general latent attack to demonstrate the controllability and feasibility of our attack. We also demonstrate the stealthiness (semantic similarity) of the perturbed instance for our attack, compared with general latent-based attacks.

We use a Convolutional Neural Network for the encoder, a Deconvolutional Neural Network for the decoder and a Multi-Layer Perceptron (MLP) for the discriminator and classifier in CF-VAE for experiments on all data sets. We use [0,1] normalised data as targets for the mean of a Bernoulli distribution, using negative cross-entropy for $\log p(x|z)$ and Adam optimiser with learning rate 10^{-4} , $\beta_1 = 0.9$; $\beta_2 = 0.999$ for the VAE updates, as in [5]. We also use Adam for the discriminator updates with $\beta_1 = 0.5$; $\beta_2 = 0.9$ and a learning rate tuned from $\{10^{-4}, 10^{-5}\}$. We use 10^{-4} for MNIST, and 10^{-5} for CelebA. The encoder outputs parameters for the mean and log-variance of Gaussian $q(z|x)$, and the decoder outputs logits for each entry of the image. We use the same six layer MLP discriminator with 1000 hidden units per layer and leaky ReLU (lReLU) nonlinearity, that outputs two logits in all CF-VAE experiments, as in [6]. We train for 3×10^5 iterations on MNIST and 10^6 iterations on CelebA. We use a batch size of 200 for all data sets. The default hurdle values to recognize satisfactory adversarial example are $[\theta_{FR} = 0.2, \theta_{SSIM} = 52, \theta_{ER} = 0.1, \epsilon = 0.1]$.

5.4 Evaluations

In this section, we present and explain the high vulnerability of DNN classifiers to our semantic adversarial attack under various settings and demonstrate the perturbation stealthiness and universality as well.

5.4.1 Evaluation Vulnerability to Adversarial Attack Under Various Settings

To demonstrate performance of our semantic adversarial attack, we first compare such attack with other types of attacks, namely *latent* (perturbation is conducted generally into latent representations derived from autoencoder or inverter, e.g., natural adversarial example [3]), *semantic* (perturbation is conducted into disentangled latent representations derived from CF-VAE) and *boosted semantic* (perturbation is conducted into disentangled latent representations derived from CF-VAE+GAN-B) settings respectively.

Attack Performance and Robustness. We apply our adversarial attack to some state-of-the-art black-box classifiers for images, i.e. two-layer LeNet [27] convolutional neural

network classifier for MNIST (with 99.1% accuracy), 50-layer ResNet [28] classifier for CelebA face (81.3% accuracy for identification classifier).

For each perturbation procedure and its corresponding setting, we evaluate the adversarial attack with each selected class. The attack SR on the test set is calculated for each class.

Effect of Parameters. In this section, we evaluate the effect of changing hyperparameters of the scheme on the results of images. Three scenarios are evaluated, e.g., the SR performance for **ordinary latent** (legend latent), general SR performance for **semantic** (legend semantic, in this case, we define a successful adversarial example when misclassification is achieved by perturbing any latent factor), and factor-specific SR performance for **semantic** (legend factor-n, in this case, we define a successful adversarial example when misclassification is achieved by only perturbing a specific latent factor). An adversarial example candidate is decided as a satisfactory (or successful) adversarial example when the perturbation added to the latent factor(s) within a value range can achieve misclassification, while the efficient ratio ER and its structural similarity SSIM (or other similarity evaluation) are both more than thresholds θ_{ER} and θ_{SSIM} respectively.

Therefore, we evaluate the SR change when varying the hurdle for ER and similarity evaluations (e.g., structural similarity SSIM, distance in latent space DLS and pHash similarity hurdles) respectively. We also investigate how the perturbation value range distribution over satisfactory adversarial examples in terms of the SR.

As shown in the first subfigure of Fig. 5, the attack SR generally decreases when we increase the hurdle of ER to decide an adversarial example. In comparison, we can achieve a generally more decent attack performance with a high SR (more than 80% for factor-specific evaluation even 100% for general evaluation when ER hurdle is set as 10%) compared with an ordinary latent attack (0% SR when ER hurdle is set as 10%) as ER hurdle increases. Note that the SR will tend to be 0% when the hurdle of ER is set more than a relatively large value (50% for the semantic latent attack while 5% for ordinary latent attack).

The second to fourth subfigures of Fig. 5 describes the impacts of the similarity hurdle on the SR change. Generally, a great SSIM similarity or a small pHash and DLS similarity values reveal a good quality of the adversarial examples. When we raise the hurdle of SSIM evaluation or reduce the hurdle of pHash and DLS evaluations to decide an adversarial example, the attack SR generally declines. Namely, when we improve the desired quality criteria of adversarial examples, the number of satisfactory adversarial examples will decrease (it is harder to find satisfactory adversarial examples). Again, our attack can achieve an overall better attack performance as the criterion of similarity for satisfactory adversarial examples increases, compared with the ordinary latent attack.

We also demonstrate the impact of choosing various perturbation value ranges on the SR, namely how the perturbations of adversarial examples distribute over satisfactory adversarial examples. In order to conduct the semantic adversarial attack, an array of perturbations is added to various latent factors by varying the value range of fac-

tors exponentially from -10 to 10. As shown in the last subfigure of Fig. 5, most adversarial examples candidates are defined as satisfactory adversarial examples using the perturbation within a small perturbation range value for ordinary latent attacks, while the perturbation values that achieve satisfactory semantic adversarial examples are more evenly distributed. The reason is that the goal of ordinary latent attacks is to find the minimum perturbations that can cause misclassification only, no matter how the adversarial example differs from the original one in terms of some similarity metrics. However, our semantic attack aims to find appropriate perturbations that can cause misclassification via controlling specific feature(s), in which many determinants can affect the value range locating, e.g., the stealthiness in both the latent and input space. On the other hand, such range value distribution figures can provide a precise “handbook” for adversarial to design effective perturbation of adversarial attack, which can be experimentally obtained using a similar dataset as the targeted data.

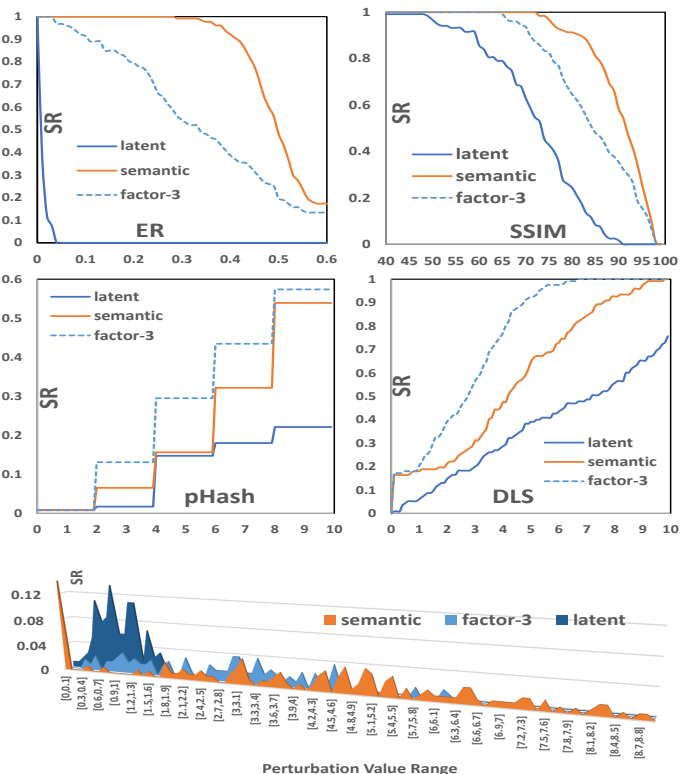


Fig. 5. Success rate evaluation. The first two rows reveal the SR change when varying hurdle of efficient ratio ER, similarity evaluation metric, e.g., structural similarity SSIM, pHash similarity and distance in latent space similarity. The last figure demonstrates the success rate achieved on various perturbation range value.

Effect of Selected Latent Factors. Next, we will demonstrate the impact of selected latent factors on the SR in the following parts in detail. We evaluate the SR change when varying the hurdle for ER and similarity evaluations (e.g., structural similarity SSIM, distance in latent space DLS and pHash similarity hurdles) respectively, perturbing only one latent factor for each attack round. We also investigate how the perturbations of adversarial examples distribute over satisfactory adversarial examples when varying the latent factor to be perturbed.

As shown in Fig. 6, when we change the hurdle of ER, SSIM similarity, pHash, and DLS similarity values to decide an adversarial example, all factors have the same change tendency of attack SR. However, these detailed amplitudes of variation are different. Various factors show better performances in terms of SR at different hurdle criteria as well as different hurdle value ranges. Consequently, based on the experimental analysis in Fig. 5 and Fig. 6, the attacker can choose one appropriate factor to conduct the attack and choose the efficient value range for the selected features in terms of attack SR. We demonstrated the robustness of our attack against strong defenses in Fig. 5 and Fig. 6. The varying threshold of distance in the latent space (DLS) is used to reveal different levels of distinguishability of defenses.

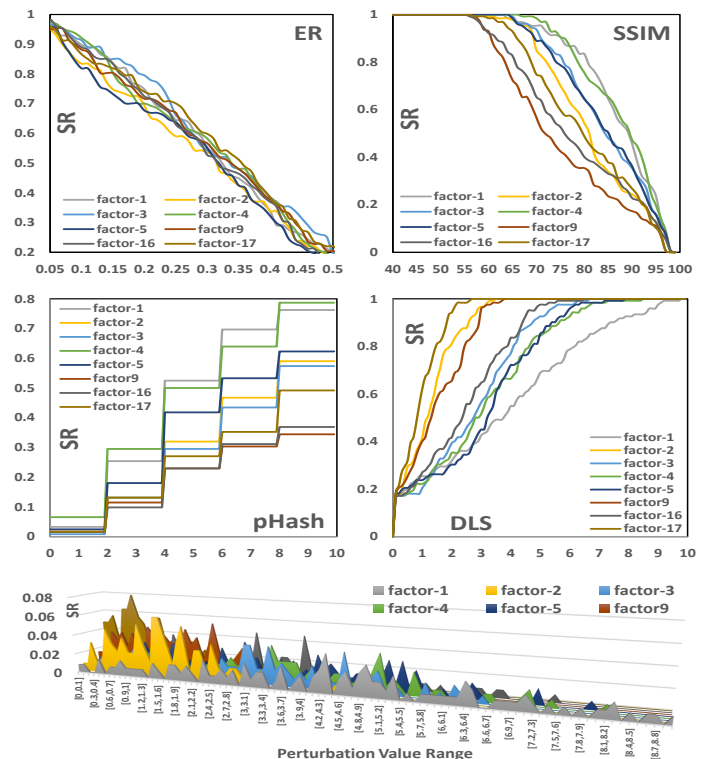


Fig. 6. Success rate evaluation when perturbing different latent factor. The first two rows reveal the success rate change when varying hurdle of efficient ratio ER, similarity evaluation metric, e.g., structural similarity SSIM, pHash similarity and distance in latent space similarity. The last figure demonstrates the success rate achieved on various perturbation range value.

5.4.2 Evaluation of Perturbation Stealthiness

We compare input, ordinary, semantic and boosted perturbation generated for the five class instances. For each class, we select 100 images from class c in the testing set to implement these four perturbation mechanisms, then the average pHash, SSIM, MSE, and DLS similarity metrics are measured respectively. pHash and MSE are used to evaluate the pixel-wise similarity, DLS measures the latent similarity and SSIM estimates the similarity from the view of human cognition. The results averaged among these metrics are summarized in Table I.

We can see that *semantic* has higher SSIM similarity scores while smaller pHash, MSE and DLS based dissimi-

TABLE 1
Evaluation of Perturbation Stealthiness

Stealthiness		latent	semantic	boosted
MNIST	pHash	9.42	9.14	7.82
	MSE	0.03	0.02	0.01
	SSIM	77.20	81.85	84.32
	DLS	7.01	2.23	1.16
CelebA	pHash	39.53	18.41	16.21
	MSE	0.06	0.05	0.04
	SSIM	17.45	30.86	32.34
	DLS	8.32	5.97	5.24

larity scores (e.g., 81.5%, 9.14, 0.02 and 2.23 over MNIST), compared with the original latent attack (e.g., 77.2%, 9.42, 0.03 and 7.01 over MNIST). The results reveal that our attack can generate adversarial examples with better quality in both input space and latent space to fool a time-limited human: the stealthiness of the perturbation is better ensured by our attack. We also find that the image with a *boosted* strategy has a higher SSIM and smaller pHash, MSE and DLS dissimilarity values than that of the *semantic* perturbation. This shows that the GAN-B improves the reconstruction quality in both input space and latent space. Namely, GAN-B can further enhance the perturbation of our attack.

Similarly, the evaluations on the CelebA face data confirm these results again. We can see that *semantic* has higher SSIM similarity scores while smaller pHash, MSE and DLS based dissimilarity scores (e.g., 30.86%, 8.14, 0.05 and 18.41 over CelebA), compared with the original latent attack (e.g., 17.45%, 8.32, 0.06 and 39.53 over CelebA). The image with the *boosted* strategy has a higher SSIM and smaller pHash, MSE and DLS dissimilarity values than that of the *semantic* perturbation. Note that the similarity scores for face data are worse than hand-written digits. The reason is that the latent features of the face are more complete than digits, which requires more well-labeled data and deeper neural networks to obtain better disentangled and reconstruction performance.



Fig. 7. Demonstration of stealthiness for our attack over MNIST. An ordinary latent attack is demonstrated in the yellow box (left is the clean instance and right is the perturbed instance that causes misclassification). A semantic attack is demonstrated in the red box (left is the clean instance, middle is a perturbed instance using semantic attack and right is the perturbed instance using boosted semantic attack).

In addition, we also demonstrate the stealthiness of our attack. In Fig. 7, we compare the reversed instance from the perturbed latent variables for both ordinary latent attack and our semantic attack, taking produced adversarial examples for a single digit "7" as an example. The reversed instance by the ordinary latent attack is shown in the yellow box. We can see that such an attack might lead to misclassification by adding random noise into the latent variables, however, cannot control what the reversed instance looks like. In comparison, our semantic attack causes misclassification by perturbing a latent factor that only affects one

feature, thereby controlling what the reversed instance looks like. As demonstrated in the red box, the perturbed instance using the semantic attack can achieve misclassification by only perturbing the latent factor that affects the stroke of the digit, while the quality of the reversed instance is further enhanced by using the boosted strategy. We compare our semantic attack with this general latent attack in Fig. 5, 8, 10 and Table I, II to demonstrate the controllability and feasibility of our attack.

5.4.3 Evaluation of Universal Perturbation

If we find a misclassification perturbation for an instance by adding noise to a specific latent factor, for example perturbing the factor that affects the stroke of digit "7", it is natural to consider whether the same perturbation, added to perturb the same latent factor of a different digit "7" instance, could give rise to misclassification. Therefore, in this section, we investigate whether we can demonstrate the universality of our semantic adversarial examples on the instances with the same class type.

The goal is to evaluate whether the same perturbation on the same selected latent factor, leading to misclassification for a given classifier over a specific input x , can cause other instances from the same class with x to be misclassified and how many and how to be impacted by hurdle parameters. Specifically, we evaluate the universality of perturbation against two-layer LeNet classifiers on MNIST in terms of fooling rate FR. We select five class instances to obtain misclassification perturbation by only perturbing one latent factor f_i , which is composed of 500 images from the training set, i.e., on average 100 images per class, named construction set. The universal perturbation for each class on f_i is the average misclassification perturbation on all 100 instances with the same class, named testing set. For each universal perturbation for f_i , we test the fooling rate over a validation set that consists of randomly selected 100 images with the same class type. Four latent factors are selected to be evaluated using the approach in Algorithm 1.

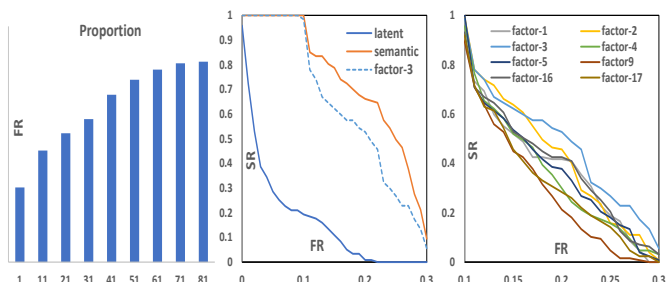


Fig. 8. Fooling rate evaluation on MNIST. The success rate SR represents the proportion of adversarial example with corresponding fooling power in terms of the fooling rate at x axis.

The first subfigure of Fig. 8 shows the fooling rates obtained on the validation set when varying the proportion of the construction set to generate universal perturbation. The fooling rate increases as the size of the proportion goes up and then tends to be stable. An interesting result is that by using an arbitrary instance of the construction set to generate universal perturbation based on our semantic attack, we can fool approximately 30% of the images on the validation set.

Next, we use the one-instance-based universal perturbation to evaluate the fooling rate, to reveal the fooling power of the instance in the construction set. The last two subfigures of Fig. 8 reveal the distribution of adversarial examples in terms of fooling rate. Overall, the universal perturbation derived from any one instance of the construction set achieves very considerable fooling rates (10 – 20%) on the validation set using our semantic latent attack. For example, more than 70% of one-instance-based universal perturbation derived from our attack scheme can fool 20% of clean images in the validation set. The fooling power of universal perturbation, derived from any one instance of the construction set using an ordinary latent attack, is generally below 10% (more than 80% one-instance-based universal perturbation). Consequently, these demonstrations reveal that our attack has remarkable universal perturbation power over unseen data points, which can be computed on a small set of training instances, even arbitrary one instance.

We further investigate the performance of the one-instance-based universal perturbation in terms of the fooling rate when varying parameter settings. As shown in the first graph in Fig. 9, we evaluate the fooling rate change when varying the hurdle for ER and similarity evaluations (e.g., structural similarity SSIM and distance in latent space DLS hurdles) respectively when figuring out perturbation over the instances in the construction set using our semantic attack. As we change the hurdle of ER, SSIM similarity and DLS similarity criteria to decide an adversarial example, the fooling rate represents different trends of change. As we increase the hurdle of efficient ratio ER, the fooling rate vibrates a lot. However, it is feasible to choose an appropriate ER hurdle that can achieve a better fooling rate. When we raise the requirement for the similarity criteria of the adversarial examples, the fooling rate will decline. We also evaluate the impact of the selected latent factor on the fooling rate when varying parameters. Various factors show good performances in terms of fooling rate at different hurdle criteria.

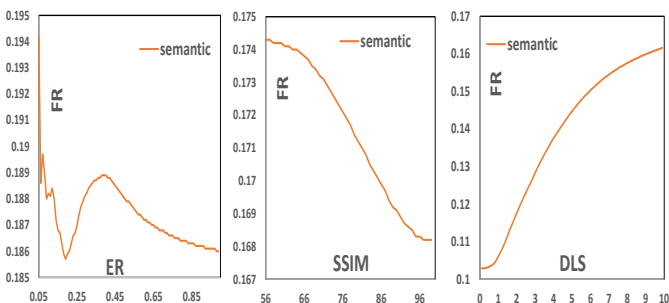


Fig. 9. Fooling rate evaluation on MNIST with varying hurdle criteria to generate adversarial examples.

We also investigate the stealthiness of the adversarial examples generated using the one-instance-based universal perturbation. The stealthiness of the results is shown in Table II.

We can see that the perturbed instances using the perturbation derived from our semantic latent attack have higher SSIM similarity scores while smaller pHash, MSE, and DLS based dissimilarity scores, compared with using the ordinary latent attack. The results reveal that the uni-

TABLE 2
Evaluation of Stealthiness for Universal Perturbation

Stealthiness		Latent	Semantic	Boosted
MNIST	pHash	19.37	12.92	10.82
	MSE	0.23	0.03	0.01
	SSIM	3.81	77.14	88.32
	DLS	7.01	0.015	0.016

versal perturbation using our attack can generate better quality adversarial examples in both input space and latent space to even fool a human. Namely, the stealthiness of the universal perturbation is better ensured by our attack. We also find that the image with *boosted* strategy can improve the reconstruction quality in both input space and latent space.

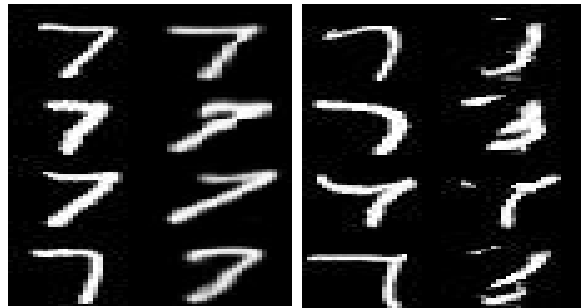


Fig. 10. Visual demonstration of stealthiness for universal perturbation. Left subfigure is the misclassified image after adding universal perturbation into a latent factor that affects angles using a semantic attack, and the right subfigure is the misclassified image after adding universal perturbation into the latent vector using the ordinary latent attack.

Fig. 10 shows a visual demonstration of the perturbed images to further demonstrate the stealthiness of the universal perturbation. Compared with the universal perturbation for ordinary latent perturbation, the universal perturbation discovered using our semantic attack is more imperceptible and stealthy. We also find that such universal perturbations are not unique, as many different efficient universal perturbations can be generated for the same value range on a given latent factor.

These experimental results show the existence of single universal perturbation, in terms of a specific latent factor, that causes clean images to be misclassified with high probability for one class of the instance. Such universal perturbations are also stealthy in both the latent and input space.

6 RELATED WORK

Since the discovery of adversarial examples for neural networks [8], researchers have found adversarial examples on various network architectures; for example, feedforward convolutional classification networks [29], generative networks [30], and recurrent networks [31]. Researchers developed several methods for generating adversarial examples, most of which leveraged gradient-based optimization from normal examples [8], [29]. Moosavi et al. showed that it was even possible to find one effective universal adversarial perturbation that, when applied, turned many images adversarial [32]. To simplify the discussion, we only focus on attacks targeting neural network classifiers.

6.0.1 Fast Gradient Sign Method (FGSM)

Given a normal image x , the fast gradient sign method [33] looks for a similar image x' in the L^∞ neighborhood of x that fools the classifier. It defines a loss function $Loss(x, l)$ that describes the cost of classifying x as label l . Then, it transforms the problem to maximizing $Loss(x', l_x)$ which is the cost of classifying image x' as its ground truth label l_x while keeping the perturbation small. The FGSM solves this optimization problem by performing a one-step gradient update from x in the image space with volume ϵ . The update step-width ϵ is identical for each pixel, and the update direction is determined by the sign of gradient at this pixel. Formally, the adversarial example x' is calculated as:

$$x' = x + \epsilon \times \text{sign}(\nabla_x \text{Loss}(x, l_x)) \quad (19)$$

Although this attack is simple, it is fast and can be quite powerful. Normally, ϵ is set to be small. Increasing ϵ usually leads to the higher attack SR.

6.0.2 Iterative Gradient Sign Method

Kurakin [34] proposed to improve FGSM by using a finer iterative optimization strategy. For each iteration, the attack performs FGSM with a smaller step-width α , and clips the updated result so that the updated image stays in the ϵ neighborhood of x . Such iteration is then repeated for several times. For the i^{th} iteration, the update process is:

$$x'_{i+1} = \text{clip}_{\epsilon, x}(x'_i + \alpha \times \text{sign}(\nabla_x \text{Loss}(x, l_x))) \quad (20)$$

This updated strategy can be used for both L1 and L2 metrics and greatly improves the SR of FGSM attack.

6.0.3 DeepFool

DeepFool is also an iterative attack but formalizes the problem differently [35]. The basic idea is to find the closest decision boundary from a normal image x in the image space, and then to cross that boundary to fool the classifier. It is hard to solve this problem directly in the high-dimensional and highly non-linear space in neural networks. So instead, it iteratively solves this problem with a linearized approximation. More specifically, for each iteration, it linearizes the classifier around the intermediate x' and derives an optimal update direction on this linearized model. It then updates x' towards this direction by a small step α . By repeating the linearize-update process until x' crosses the decision boundary, the attack finds an adversarial example with small perturbation.

6.0.4 Carlini Attack

Carlini recently introduced a powerful attack that generates adversarial examples with small perturbation [29]. The attack can be targeted or untargeted for all three metrics L^0 , L^2 , and L^∞ . We take the untargeted L^2 version as an example here to introduce its main idea. We may formalize the attack as the following optimization problem:

$$\text{minimize } \|\delta\|_2 + c \times f(x + \delta) \text{ s.t. } x + \delta \in [0, 1]^n \quad (21)$$

For a fixed input image x , the attack looks for a perturbation δ that is small in length and fools the classifier (the $f()$ term in objective) at the same time. c is a hyperparameter

that balances the two. Also, the optimization has to satisfy the box constraints to be a valid image. $f()$ is designed in such a way that $f(x') \leq 0$ if and only if the classifier classifies x' incorrectly, which indicates that the attack succeeds. $f(x')$ has hinge loss form and is defined as

$$f(x') = \max(Z(x')_{l_x} - \max\{Z(x')_i : i \neq l_x\}, -\kappa) \quad (22)$$

where $Z(x')$ is the pre-softmax classification result vector (called logits) and l_x is the ground truth label. κ is a hyper-parameter called confidence. Higher confidence encourages the attack to search for adversarial examples that are stronger in classification confidence. High-confidence attacks often have larger perturbations and better transferability.

One strong defense is to detect or purify input data that may have added adversarial perturbation with hand-crafted statistical features [36], separate classification networks [37] or detector-based denoising [38]. MagNet [38], one or more separate detector networks and a reformer network are used to defend adversarial examples. The detector networks learn to differentiate between normal and adversarial examples by approximating the manifold of normal examples. The reformer network passes input data to the autoencoders that move input data closer to the data manifold.

To address the unnatural perturbations added into the input space, [3] applies GAN to generate natural and legible adversarial examples that lie on the data manifold, by searching in semantic space of dense and continuous data representation. It aims to solve the mismatch between the input space perturbation and the semantic space features. However, the perturbations in the latent space are hard to control due to the lack of interpretability and factorization/disentanglement.

To the best of our knowledge, this is the first work that introduces a systematic framework to generate semantic adversarial examples that are designed by perturbing the disentangled latent variables in an interpretable, practical and stealthy manner.

7 CONCLUSION AND DISCUSSION

In this paper, we propose a practical semantic adversarial attack scheme to produce adversarial examples that can be designed in a human-cognition manner with structured perturbations with semantic meanings. We implement such an attack against black-box classifiers for images. Specifically, we propose onefold and multiple semantic feature manipulation approaches, respectively. For the onefold scenario, we propose the CF-VAE to obtain disentangled latent representation that can easily be manipulated in an interpretable manner. The disentanglement performance is improved from two aspects: driving the label relevant information from latent factors and improving the inner independence of latent factors. In addition, a GAN-B is applied to use the representation similarity derived from the discriminator of GAN to evaluate the reconstruction error so that it addresses the trade-offs between reconstruction and disentanglement. An invisible perturbation mechanism is proposed to find the most efficient latent factors to conduct the perturbation that causes misclassification while ensuring the stealthiness. For multiple scenarios, we apply an image-to-image transition

to jointly train two CF-VAE that can produce more precise constraints on the reconstructed images using natural target images.

Our detailed experiments demonstrate that our attack schemes are both stealthy and efficient to generate adversarial examples in an interpretable and smooth manner while ensuring the stealthiness of malicious perturbation in both a visual perspective and latent space. We also demonstrate that universal semantic adversarial examples exist in a significant number of samples with the same labels. As the learned latent feature vector is disentangled, we provide a perturbation design handbook for adversarial attacks to show which factor affects which feature and how much. Thus, two or more latent factors will affect corresponding factorized features, respectively. The quality of the reconstructed image is not significantly affected by how many features are changed but how much perturbation is applied to individual features. After obtaining the perturbation design handbook, our attack can decide the perturbation for infinite instances in one-shot (constant time). Most existing adversarial attacks design perturbation for each instance one by one. Therefore, our attack is highly efficient by construction and experiments for a time-based comparison are not necessary.

A potential refinement of our work includes designing universal perturbation for multiple classifiers and targeted misclassification and further addressing the disentanglement and reconstruction trade-off. We also aim to investigate applying variants of the semantic attack to other domains besides image classification, e.g., time-series data and text data. In addition, we will continue to improve the disentanglement performance and explore class-unique features.

REFERENCES

- [1] N. Papernot, P. McDaniel, S. Jha, M. Fredrikson, Z. B. Celik, and A. Swami, "The limitations of deep learning in adversarial settings," in *Security and Privacy (EuroS&P), 2016 IEEE European Symposium on*. IEEE, 2016, pp. 372–387.
- [2] Y. Liu, X. Chen, C. Liu, and D. Song, "Delving into transferable adversarial examples and black-box attacks," *arXiv preprint arXiv:1611.02770*, 2016.
- [3] Z. Zhao, D. Dua, and S. Singh, "Generating natural adversarial examples," *arXiv preprint arXiv:1710.11342*, 2017.
- [4] A. B. L. Larsen, S. K. Sønderby, H. Larochelle, and O. Winther, "Autoencoding beyond pixels using a learned similarity metric," *arXiv preprint arXiv:1512.09300*, 2015.
- [5] I. Higgins, L. Matthey, A. Pal, C. Burgess, X. Glorot, M. Botvinick, S. Mohamed, and A. Lerchner, "beta-vae: Learning basic visual concepts with a constrained variational framework," in *International Conference on Learning Representations*, vol. 3, 2017.
- [6] H. Kim and A. Mnih, "Disentangling by factorising," *arXiv preprint arXiv:1802.05983*, 2018.
- [7] Y. Bengio, A. Courville, and P. Vincent, "Representation learning: A review and new perspectives," *IEEE transactions on pattern analysis and machine intelligence*, vol. 35, no. 8, pp. 1798–1828, 2013.
- [8] C. Szegedy, W. Zaremba, I. Sutskever, J. Bruna, D. Erhan, I. Goodfellow, and R. Fergus, "Intriguing properties of neural networks," *arXiv preprint arXiv:1312.6199*, 2013.
- [9] B. Biggio, I. Corona, D. Maiorca, B. Nelson, N. Šrndić, P. Laskov, G. Giacinto, and F. Roli, "Evasion attacks against machine learning at test time," in *Joint European conference on machine learning and knowledge discovery in databases*. Springer, 2013, pp. 387–402.
- [10] X. Chen, Y. Duan, R. Houthoofd, J. Schulman, I. Sutskever, and P. Abbeel, "Infogan: Interpretable representation learning by information maximizing generative adversarial nets," in *Advances in neural information processing systems*, 2016, pp. 2172–2180.
- [11] J. Donahue, P. Krähenbühl, and T. Darrell, "Adversarial feature learning," *arXiv preprint arXiv:1605.09782*, 2016.
- [12] A. Kumar, P. Sattigeri, and P. T. Fletcher, "Improved semi-supervised learning with gans using manifold invariances," *Advances in Neural Information Processing Systems (NIPS)*, 2017.
- [13] C. Ledig, L. Theis, F. Huszár, J. Caballero, A. Cunningham, A. Acosta, A. Aitken, A. Tejani, J. Totz, Z. Wang et al., "Photo-realistic single image super-resolution using a generative adversarial network," in *2017 IEEE Conference on Computer Vision and Pattern Recognition (CVPR)*. IEEE, 2017, pp. 105–114.
- [14] S. Reed, Z. Akata, X. Yan, L. Logeswaran, B. Schiele, and H. Lee, "Generative adversarial text to image synthesis," *arXiv preprint arXiv:1605.05396*, 2016.
- [15] S. Watanabe, "Information theoretical analysis of multivariate correlation," *IBM Journal of research and development*, vol. 4, no. 1, pp. 66–82, 1960.
- [16] M.-Y. Liu, T. Breuel, and J. Kautz, "Unsupervised image-to-image translation networks," in *Advances in neural information processing systems*, 2017, pp. 700–708.
- [17] X. Huang, M.-Y. Liu, S. Belongie, and J. Kautz, "Multimodal unsupervised image-to-image translation," in *Proceedings of the European Conference on Computer Vision (ECCV)*, 2018, pp. 172–189.
- [18] Z. Liu, P. Luo, X. Wang, and X. Tang, "Deep learning face attributes in the wild," in *Proceedings of International Conference on Computer Vision (ICCV)*, December 2015.
- [19] A. Makhzani, J. Shlens, N. Jaitly, I. Goodfellow, and B. Frey, "Adversarial autoencoders," *arXiv preprint arXiv:1511.05644*, 2015.
- [20] L. A. Gatys, A. S. Ecker, and M. Bethge, "A neural algorithm of artistic style," *arXiv preprint arXiv:1508.06576*, 2015.
- [21] Z. Wang, E. P. Simoncelli, and A. C. Bovik, "Multiscale structural similarity for image quality assessment," in *The Thirty-Seventh Asilomar Conference on Signals, Systems Computers*, 2003, vol. 2, 2003, pp. 1398–1402 Vol.2.
- [22] J.-Y. Zhu, T. Park, P. Isola, and A. A. Efros, "Unpaired image-to-image translation using cycle-consistent adversarial networks," in *Proceedings of the IEEE international conference on computer vision*, 2017, pp. 2223–2232.
- [23] Y. LeCun, C. Cortes, and C. Burges, "Mnist handwritten digit database," *ATT Labs [Online]*. Available: <http://yann.lecun.com/exdb/mnist>, vol. 2, 2010.
- [24] Y. LeCun, L. Bottou, Y. Bengio, P. Haffner et al., "Gradient-based learning applied to document recognition," *Proceedings of the IEEE*, vol. 86, no. 11, pp. 2278–2324, 1998.
- [25] Z. Liu, P. Luo, X. Wang, and X. Tang, "Deep learning face attributes in the wild," in *Proceedings of the IEEE international conference on computer vision*, 2015, pp. 3730–3738.
- [26] C. Liao, H. Zhong, A. Squicciarini, S. Zhu, and D. Miller, "Backdoor embedding in convolutional neural network models via invisible perturbation," *arXiv preprint arXiv:1808.10307*, 2018.
- [27] Y. LeCun, P. Haffner, L. Bottou, and Y. Bengio, "Object recognition with gradient-based learning," in *Shape, contour and grouping in computer vision*. Springer, 1999, pp. 319–345.
- [28] K. He, X. Zhang, S. Ren, and J. Sun, "Deep residual learning for image recognition," in *Proceedings of the IEEE conference on computer vision and pattern recognition*, 2016, pp. 770–778.
- [29] N. Carlini and D. Wagner, "Towards evaluating the robustness of neural networks," in *2017 IEEE Symposium on Security and Privacy (SP)*. IEEE, 2017, pp. 39–57.
- [30] J. Kos, I. Fischer, and D. Song, "Adversarial examples for generative models," in *2018 IEEE Security and Privacy Workshops (SPW)*. IEEE, 2018, pp. 36–42.
- [31] N. Papernot, P. McDaniel, A. Swami, and R. Harang, "Crafting adversarial input sequences for recurrent neural networks," in *Military Communications Conference, MILCOM 2016-2016 IEEE*. IEEE, 2016, pp. 49–54.
- [32] S.-M. Moosavi-Dezfooli, A. Fawzi, O. Fawzi, and P. Frossard, "Universal adversarial perturbations," in *2017 IEEE Conference on Computer Vision and Pattern Recognition (CVPR)*. Ieee, 2017, pp. 86–94.
- [33] I. J. Goodfellow, J. Shlens, and C. Szegedy, "Explaining and harnessing adversarial examples (2014)," *arXiv preprint arXiv:1412.6572*.
- [34] A. Kurakin, I. Goodfellow, and S. Bengio, "Adversarial examples in the physical world," *arXiv preprint arXiv:1607.02533*, 2016.
- [35] S.-M. Moosavi-Dezfooli, A. Fawzi, and P. Frossard, "Deepfool: a simple and accurate method to fool deep neural networks," in

Proceedings of the IEEE Conference on Computer Vision and Pattern Recognition, 2016, pp. 2574–2582.

- [36] K. Grosse, P. Manoharan, N. Papernot, M. Backes, and P. McDaniel, “On the (statistical) detection of adversarial examples,” *arXiv preprint arXiv:1702.06280*, 2017.
- [37] J. H. Metzen, T. Genewein, V. Fischer, and B. Bischoff, “On detecting adversarial perturbations,” *arXiv preprint arXiv:1702.04267*, 2017.
- [38] D. Meng and H. Chen, “Magnet: a two-pronged defense against adversarial examples,” in *Proceedings of the 2017 ACM SIGSAC Conference on Computer and Communications Security*. ACM, 2017, pp. 135–147.